A CHRONOSTRATIGRAPHIC FRAMEWORK FOR THE NORTHWESTERN SLOPE OF THE GULF OF MEXICO

A Thesis

by

KRISTEN EILEEN ELSTON

Submitted to the Office of Graduate Studies of
Texas A&M University
in partial fulfillment of the requirements for the degree of

MASTER OF SCIENCE

December 2005

Major Subject: Oceanography

A CHRONOSTRATIGRAPHIC FRAMEWORK FOR THE NORTHWESTERN SLOPE OF THE GULF OF MEXICO

A Thesis

by

KRISTEN EILEEN ELSTON

Submitted to the Office of Graduate Studies of
Texas A&M University
in partial fulfillment of the requirements for the degree of

MASTER OF SCIENCE

Approved by:

Chair of Committee,	Niall Slowey
Committee Members,	Ethan Grossman
	William Bryant
Head of Department,	Wilford Gardner

December 2005

Major Subject: Oceanography

ABSTRACT

A Chronostratigraphic Framework for
the Northwestern Slope of the
Gulf of Mexico. (December 2005)
Kristen Eileen Elston, B.S., Texas A&M University
Chair of Advisory Committee: Dr. Niall C. Slowey

Sediments from two cores, JPC31 and JPC46, were analyzed to better understand the relationship between climate and sediment deposition on the continental slope of the northwestern Gulf of Mexico. These two cores were selected from a suite of cores collected from the slope of the Gulf of Mexico after examining how bulk density varied with depth in the cores. The presence/absence of *Globoratalia menardii*, down-core variations of the $\delta^{18}O$ of *Globigerinoides ruber*, tephrochronology, and radiocarbon dating of *G. ruber* were used to determine the chronologies of the sediments in the cores. *Globorotalia menardii* were present until a depth of 100 cm in JPC31. The entrance of *G. menardii* in the Gulf of Mexico was dated at 8 kyr. Analysis of an ash layer found in both JPC31 and 46 yielded a date of 84 kyr, at depths of 700 cm and 1440 cm, respectively. Radiocarbon dating yielded four ages in JPC31. In sediment core JPC31, Marine Isotope Stage (MIS) 1-5 were recorded. In sediment core JPC46, MIS 2-4 and a portion of MIS 5 were recorded.

These results provide a framework for determining general sedimentation rates from the northwestern slope of the Gulf of Mexico. Events in the density profiles in JPC31 and JPC46 were correlated to corresponding events in the rest of the slope cores, allowing the chronologies of JPC31 and JPC46 to be transferred to the suite of the slope cores. Sedimentation rates along different portions of the slope were then calculated, and variations in these sedimentation rates were used to better understand slope sedimentary processes.

Sedimentation rates on the northwestern slope of the Gulf of Mexico were calculated for the most recent 120,000 years and compared with climate to deduce trends. Sedimentation rates for MIS 1-5 ranged from 7 cm/kyr to 28 cm/kyr. The sedimentation rate for the last glaciation (MIS 2, 3, and 4) were the highest for the time interval studied. The lowered sea level during glacial advances brings sediments farther out onto the slope; therefore, a higher sedimentation rate is expected during this time. These rates varied from 22 cm/kyr near the coast to 7 cm/kyr toward the abyssal plains. Of the 12 cores analyzed along the slope, JPC23 and JPC24 had the lowest sedimentation rates. This is likely due to high density bottom currents and turbidity currents which carry sediments farther out on the slope. Therefore, the lowest sedimentation rates would be expected a great distance from the land mass and some distance from the abyssal plains.

DEDICATION

This thesis is dedicated to the graduate students of the Oceanography Department from whom I learned a world beyond Texas A&M University while eating lunch and without whom I would not have met my husband.

ACKNOWLEDGEMENTS

My thanks and gratitude to my committee members Niall Slowey, Ethan Grossman and Bill Bryant. Thank you for your time and help in the last six years. My sincere appreciation to Niall Slowey, my committee chair, who has seen me through my thesis work. I can't thank him enough for his time as well as his friendship.

Many thanks to Sandy Drews and Marilyn Yeager, my biggest supporters and wonderful friends who always gave great advice. Dan Bean, Debora Berti and Efthymios Trispsanas were a great help with demonstrating techniques and mapping problems.

Thanks to my dear friend Amy Bratcher for letting me live in her house for a semester and always welcoming me on her couch.

Thank you to my parents for love and support in the last 28 years of my life. Thank you to my husband for cooking as I wrote and for his reminders that often prompted phone calls to my advisor.

Many thanks go to the Department of Geology and Geophysics for allowing me to use the mass spectrometer, as well as the Electron Microprobe.

The collection of these cores was sponsored by a National Science Foundation grant to Texas A&M (No. BES-9530370) with supplemental support from Chevron, Mobil, Texaco, Phillips, Marathon, and MARSCO Inc.

TABLE OF CONTENTS

LIST OF TABLES

LIST OF FIGURES

CHAPTER I
INTRODUCTION

The continental slope of the Gulf of Mexico is one of the most complex in the world. Salt diapirism strongly influences the slope with active movement of sediments as basins and ridges are formed and others are buried (Bryant and Liu, 2000; Amery, 1969; Gealy, 1955). Much of the attention paid to the geology of the slope of the Gulf of Mexico has been to study the formation of the basins, ridges and influence of the Mississippi River (Bryant and Liu, 2000; Amery, 1969; Gealy, 1955). As the petroleum industry continues to move farther from the shore, there is a growing need to understand sedimentological processes. Fundamental knowledge about sedimentary processes is best obtained through the creation of an age model, which can be applied to both climate and sea level.

The climate of the last 20,000 years has also been the subject of much research. The end of the Pleistocene was dominated by the last glacial maximum from about 22,000 to 14,000 BP (see review by Crowley and North, 1991). Estimated sea-level at that time was about 120 meters below today's sea level (Fairbanks, 1989). Upon deglaciation, glacial melt water and sediments traveled down the Mississippi River into the Gulf of Mexico (Broecker et al., 1989). During glacial periods, the lighter isotope, ^{16}O, is preferentially stored on land in glaciers, enriching the residual ocean in the heavier isotope, ^{18}O. Due to cooler temperatures and enriched ^{18}O, foraminifera that live during glacial periods will incorporate more ^{18}O into their shells than foraminifera that live during interglacial periods. Shells deposited on the shelf exhibit recognizable patterns of $^{18}O/^{16}O$. Marine oxygen isotope stages are defined by a pattern of high and low $^{18}O/^{16}O$ (Emiliani, 1955, Shackleton and Opdyke, 1973). For the entire Quaternary, 63 stages have been identified by Ruddiman et al. (1986).

This thesis follows the style and format of Marine Geology.

Due to the recognizable patterns of $\delta^{18}O$, these results can be used to estimate sediment ages (Shackleton and Opdyke, 1973). Additionally, radiocarbon dating (Bard, 1988) and tephrochronology (Sarna-Wojcicki, 2000) also provide ages of sediments to develop a chronostratigraphy. Finally, the most recent entrance of *Globorotalia menardii* into the Gulf of Mexico also provides an absolute date.

In this study we have created a basic age model for recent sedimentation on the northwestern slope of Gulf of Mexico and determined sediment horizons into context of climate and sea level change. By using oxygen isotopes and other methods of stratigraphy, I described the recent geochronology of the northwestern slope of the Gulf of Mexico and provided a framework for others to use. The information yielded by this research is both practical and applicable to geological engineering purposes on the slope of the Gulf of Mexico.

Study Area and Field Sampling

The slope of the northwest Gulf of Mexico is among the broadest in the oceans, ranging from about 100 to 230 km wide. Its slope angle is near one degree, and it spans a water depth range of about 1000 to 2500 m (Bryant and Liu, 2000). The morphology of the slope is dominated by over one hundred domes, basins and intra-basin ridges which result from the movement of thick, underlying salt deposits (Bouma and Bryant, 1994).

Sea-level, riverine sediment input, and ocean surface waters, along with faulting and geomorphology, all influence sedimentation on the ocean floor. Because of the high sea-level stand today, the distance from the shoreline to the slope is great; the sediments on the slope are hemipelagic (Bryant et al., 1995) and heavily bioturbated (Bryant and Liu, 2000). Sedimentation rates in the area are commonly expected to be around 10 cm per 1000 years, with some variation due to sea level and climate change. Because of these relatively high rates, these sediments potentially preserve a valuable record of past climate and other environmental conditions.

In August of 1998, the R/V Knorr (cruise 159) collected a suite of jumbo piston cores near Bryant Canyon on the northwestern slope of the Gulf of Mexico (Figure 2)

using the WHOI Jumbo Piston Corer. In order to understand sedimentation in this area, these cores were taken at several locations including the high stable ridges, the basin floors and within the canyon itself. Each core was logged for density, compressional-wave velocity, and magnetic susceptibility using a GEOTEK Multi-Sensor Core Logger, at 2 cm intervals. All of these cores show a similar density pattern. The pattern noted through the cores selected is that of a gradual increase followed by a spike through the continued increase, a trough, a spike, and a continuation of the gradual increase (a few representative graphs can be seen in Figure 3).

This study used cores from topographically isolated inter-basin high areas without evidence of disturbance by turbidity currents or other down-slope processes to assure that changes seen in the profiles are caused by environmental conditions, rather than slope failure, etc. Based on density profiles for the cores (Figure 3) I chose two cores to study: Jumbo Piston Core (JPC) 31 and 46. JPC 31 was retrieved at 26.41° N and 92.27° W and is closest to Chalmette, Beaumont and La Salle basins. JPC 46 was collected at 27.06° N and 92.34° W and is closest to Morgan and Calcasieu basins (Figure 1). JPC 31 was approximately 15 meters long and was chosen because of its slow sedimentation rate, which would provide the older record of the two cores. JPC 46 was approximately 17 meters long and was chosen for its high sedimentation rate, which would provide a high-resolution record. JPC 46 is approximately 17 meters long. Figure 1 shows the location of these two cores. Importantly, because these cores have downcore property profiles representative of the entire suite of cores, their chronologies are regionally applicable.

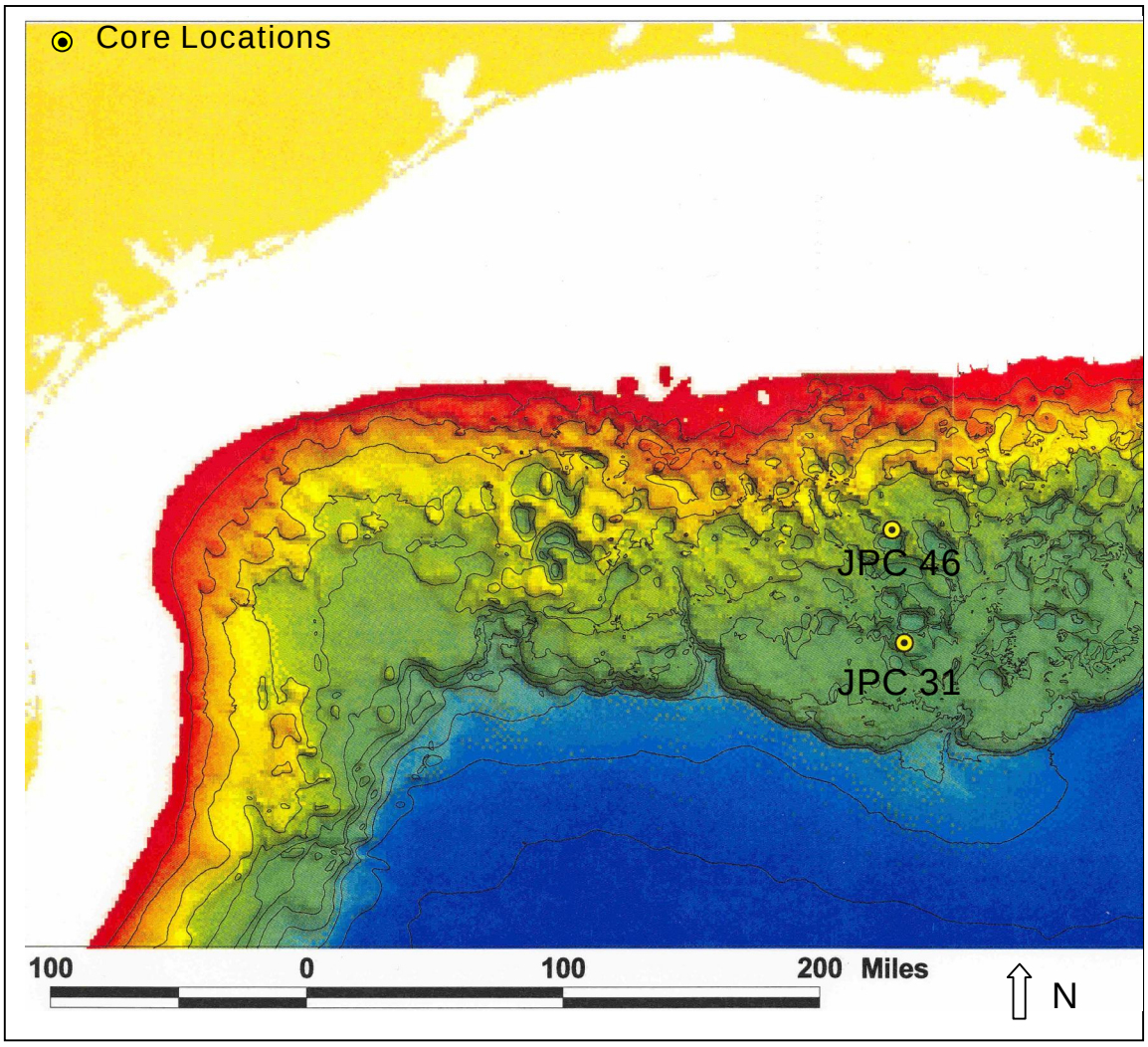

Figure 1: Map and Location of the Northwestern Slope and Study Cores. The shaded area above is the Texas and Louisiana coast.

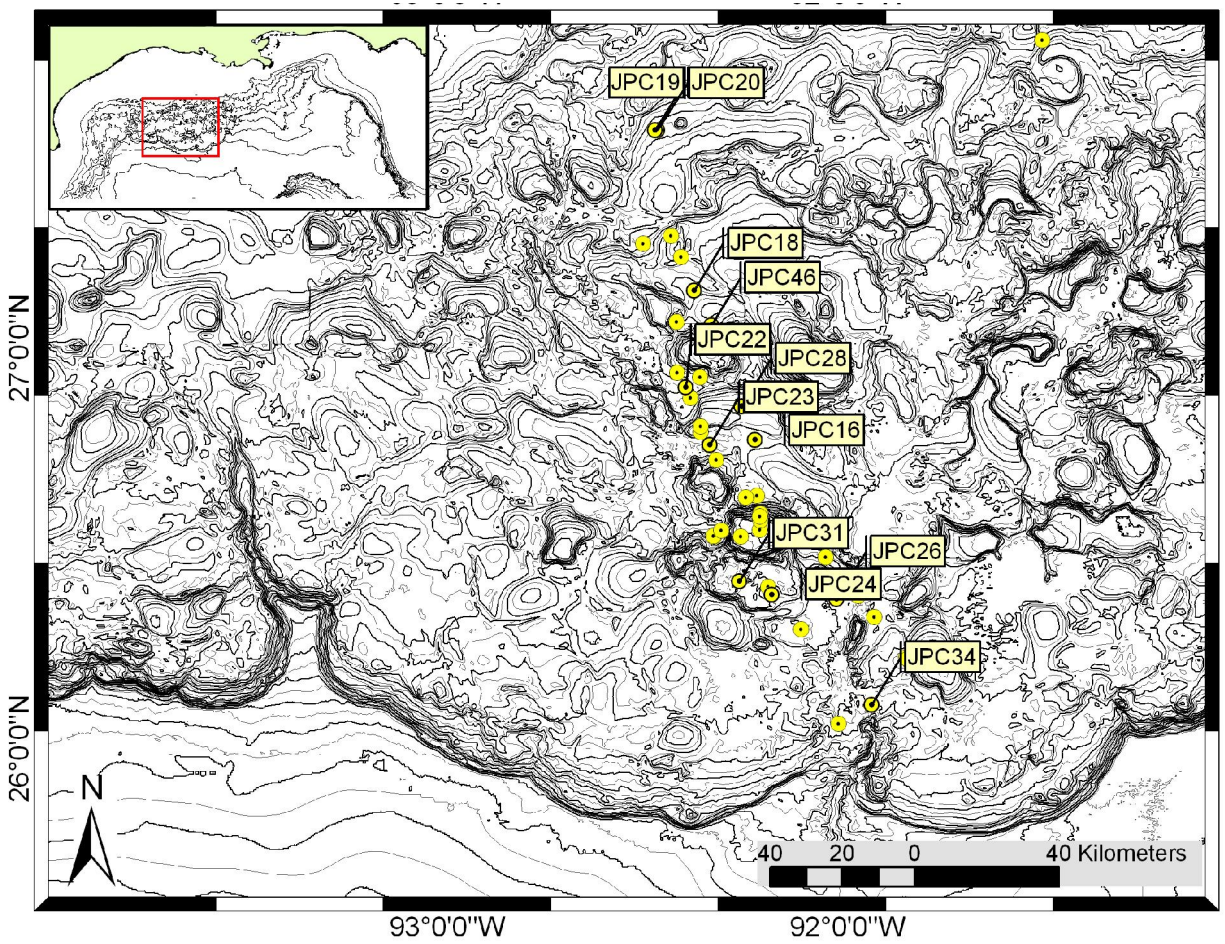

Figure 2: Map of Cores Collected on Knorr 159. Contour intervals are 50 m.

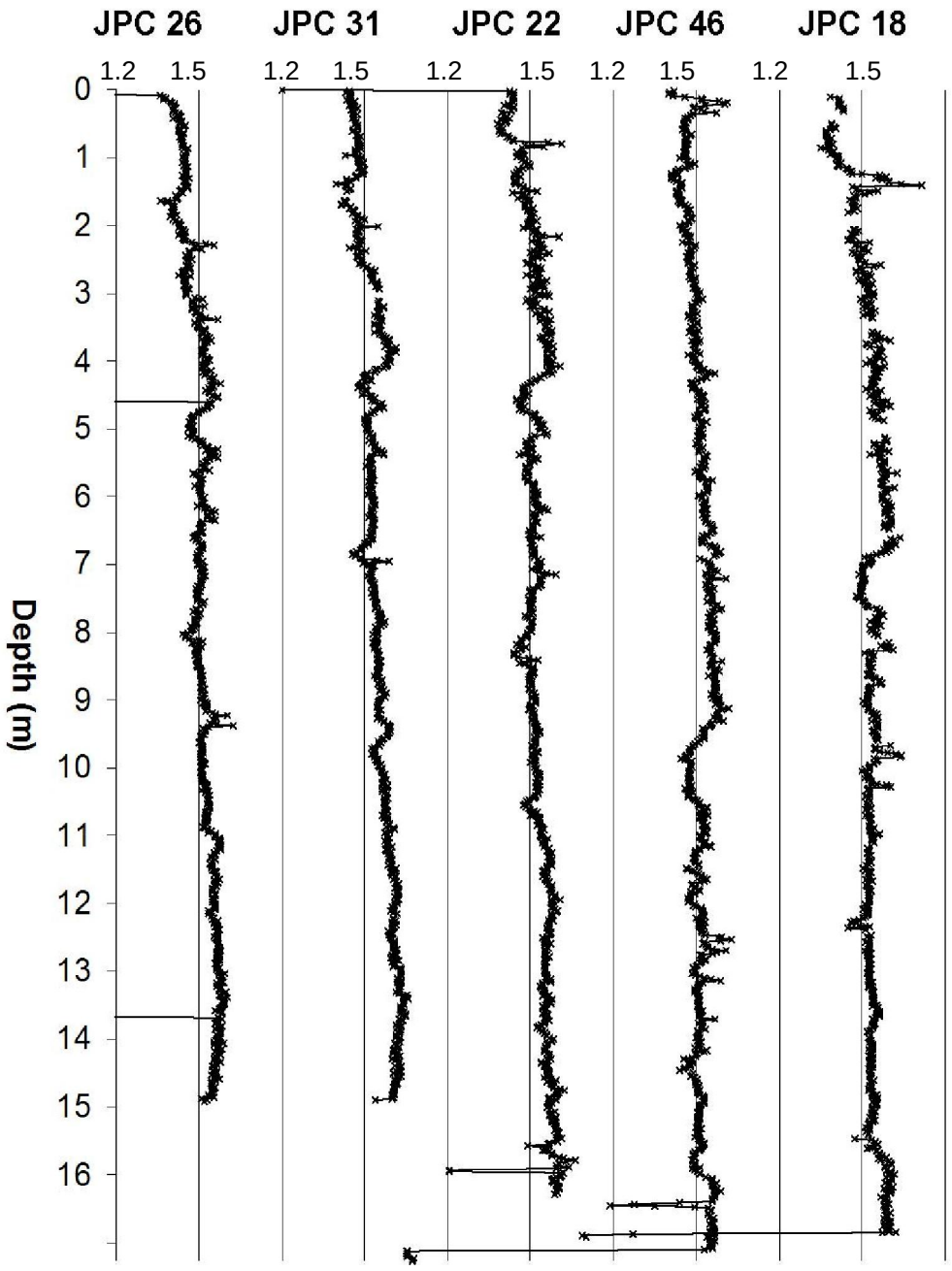

Figure 3: Density (gm/cc) Profiles of Selected Cores.

CHAPTER II
LABORATORY METHODS

Sedimentation in this area was studied through a detailed analysis of sediment cores. After JPC 31 and 46 were split, their lithologies were examined visually and described. No significant sign of erosional gaps or disturbance by down-slope mass-wasting processes, such as slumping, were apparent. Samples were then collected from the cores at 10-cm intervals. Each sample was 2 cm wide. Sediment immediately adjacent to the core liner was discarded to avoid contamination by more recent sediments smeared along the surface of the core liner during core recovery. A total dry sediment weight of approximately 20 grams was obtained. Samples were then washed through a 63 μm sieve and the >63 μm fraction was dried to determine the abundance of sand-sized particles. Foraminiferal tests were picked from the sand fraction and used to determine the chronology of the cores by the following methods: 1) *G. menardii* abundance, and 2) oxygen isotopes, and 3) ^{14}C dating. Tephrochronology and acoustic methods provided additional aids in the interpretation of the stratigraphy. All of these methods are described below.

Foraminiferal Abundances

A key species used in biostratigraphy for the Gulf of Mexico is *Globorotalia menardii*. During the late Quaternary, these planktonic foraminifera only appear in the Gulf of Mexico during interglacial stages (Ericson and Wollin, 1968; Martin et al., 1990; Emiliani, 1975). *G. menardii* inhabited these waters for approximately the most recent 8,000 years of the Holocene (Jones, 1993) and during the last interglacial interval (oxygen isotope stage 5). They do not appear during the last glaciation (oxygen isotope stages 2, 3 and 4). By determining the depth distribution of *G. menardii* in the cores, we can begin to identify the isotopic stages during which sediments in the northwestern slope of the Gulf of Mexico were deposited.

The 355-425 μm fraction of sediments from cores JPC 31 and JPC 46 was examined for the occurrence of *G. menardii*. This size fraction was used to ensure confidence in identifying the correct species for analysis and for consistency with previous studies. I determined the relative abundance qualitatively, interpreting >30 specimens per 20 grams of sand as abundant. The final depth of the appearance of *G. menardii* was noted.

Oxygen Isotopes

The foraminiferal oxygen isotope stages and their absolute dates has been well documented. Emiliani (1955) pioneered foraminiferal oxygen isotope studies using planktonic foraminifera. Since then, many studies of foraminiferal oxygen isotope ratios have shown consistent temporal patterns of variability. The isotope stages with high $^{18}O/^{16}O$ ratios are glacial periods and are designated with even numbers. The isotope stages with low $^{18}O/^{16}O$ ratios are interglacial periods and are designated with odd numbers. The SPECMAP project (Imbrie et al, 1984) used sediment cores from the Atlantic Ocean and assembled $\delta^{18}O$ and $\delta^{13}C$ data for the past 400,000 years. A generalized profile of $\delta^{18}O$ variability was developed based on data of several cores. The $\delta^{18}O$ values were then compared with the earth's astronomical cycles, including eccentricity, obliquity and precession, to achieve a more finely tuned graph that can be compared to obtain absolute ages of sediment (Table 1).

Tests of the planktonic foraminifera *Globigerinoides ruber* are abundant in the Gulf of Mexico sediments. Based on the results of Curry and Mathews (1980), the 212-255 μm fraction of each sample was selected for $\delta^{18}O$ analyses. Approximately 30 individual tests of *G. ruber* (white) were picked and cleaned in an ultrasonicator to remove detritial $CaCO_3$ from the foraminifera. The $\delta^{18}O$ and $\delta^{13}C$ of groups of at least nine *G. ruber* tests were measured using Finnigan MAT 251 with Kiel II carbonate reaction system. Approximately 400 total samples from JPC 31 and JPC 46 were analyzed for this study. Results are reported relative the PDB standard. Eight samples were analyzed for two standards to ensure accurate and precise results.

Radiocarbon Dating

Carbon-14 has been used to date sediments as old as 40,000 years. ^{14}C is incorporated into the shells of living foraminifera and upon their death, the shell is then buried with the rest of the sediments on the ocean floor and the ^{14}C begins to decay. Knowing the initial ^{14}C abundance, and the half-life of ^{14}C (5,730 years), and the amount of ^{14}C in the shell today, we are able to estimate the age of the shell. Obtaining these dates provides absolute datums with which to correlate the $\delta^{18}O$ with climatic patterns. For this analysis, approximately 1200 specimens (8 mg total) of *Globigerinoides ruber* in the size fraction of 212-250 μm are picked from a given sample. In order to obtain this quantity, ~ 40 g (dry weight) of sediment was required. Four samples were sent to Lawrence Livermore National Laboratory for analysis by accelerator mass spectrometer. Resulting age estimates were corrected for surface ocean reservoir effects and converted to calendar years BP before 1950, also known as the reservoir age (Bard, 1988; Suess and Revelle, 1957; Craig, 1957; Arnold and Anderson, 1957; Stuiver and Polach, 1977).

Tephrochronology

This method of dating involves identifying layers of ash (or tephra) and applying ages to these layers by correlating each layer with an independently dated eruption. Each eruption produces tephra with a distinct chemical composition, which allows us to identify the source (Sarna-Wojcicki, 2000). In order to obtain more accurate results, the analyses were performed on individual glass shards, rather than bulk sediment analysis. Tephra spanning the last 185,000 years has been characterized by Rabek et al. (1985) for the western Gulf of Mexico and Pacific Ocean, their results provided a framework for understanding the relationships between the ash layers in JPC 31 and 46.

In both JPC 31 and 46, a single megascopic ash layer has been identified. To determine the identity of this ash, we used a Cameca SX 50electron microprobe to determine the abundance of various elements within the ash in both cores. Because the ash is plentiful and relatively pure, no dispersants or sieves were needed. Ash was mounted in epoxy and set to dry for 24 hours. After drying, each sample was abraded

with sand paper to expose the individual glass shards. The Cameca SX50 electron microprobe analysis uses wavelength dispersive methods to separate the emissions of each chemical element. Thirty individual glass shards from each sample were analyzed and the elements analyzed include: Na, Mg, Al, Si, K, Ca, Ti, Fe, and Cl, among others. This technique was used to chemically 'fingerprint' the ash and identify its source and time of eruption. The proportions were reported relative to the U.S. Geological Survey (USGS) and compared with the compositions of ash from known eruptions (Sarna-Wojicki, 2001, personal communication). For direct comparison, I also obtained ash samples previously analyzed by Rabek et al. and the USGS using the energy dispersive electron microprobe.

CHAPTER III
RESULTS AND DISCUSSION

Chronostratigraphies of Sediment Cores

JPC 31

The downcore variations in the $\delta^{18}O$ of *G. ruber* (Figure 4) indicate that most of the sediments analyzed in core JPC 31 were deposited during the penultimate glaciation through the Holocene (MIS 1 to 6). Although JPC 31 is 15 m long, only the first 9.0 m contain sufficient foraminifera for isotopic analysis. $\delta^{18}O$ values at the uppermost ~100 cm of JPC 31 are about -1.3 ‰, which is similar to the $\delta^{18}O$ of Holocene planktonic foraminifera in the tops of other cores from the region (Flower and Kennett, 1990; Emiliani, 1975; Broecker et al., 1989). The $\delta^{18}O$ values for ~160 to ~650 cm depth are typically at least 1 ‰ greater than those for the top of JPC 31, indicating sediments deposited during the last glaciation (MIS 2 to 4). Two relative maxima of $\delta^{18}O$ occur within these glacial-aged sediments: the first, occurring from ~165 to 215 cm, corresponds to sediments deposited during the last glacial maximum (MIS 2), and the second, occurring from ~550-660 cm, corresponds to sediments deposited during MIS 4. The more negative and variable $\delta^{18}O$ from intervening depths are typical of MIS 3. From ~660 to 930 cm, the $\delta^{18}O$ values decrease to values similar to those of Holocene foraminifera, indicating sediments deposited during the last interglacial period (MIS 5). There are only a few, widely spaced $\delta^{18}O$ values for depths greater than 930 cm in JPC 31 so certain identification of isotopic stages is not possible. Still, the +0.2 ‰ value at 950 cm (immediately below the sediments from the last interglacial) is consistent with these sediments being deposited during a glacial period, possibly the penultimate glaciation (MIS 6).

Downcore changes in the occurrence of *G. menardii* provide an independent constraint on the chronology of JPC 31. As shown in Figure 4, *G. menardii* are present in the first 100 cm of JPC 31, absent from 100 to 710 cm, and they are present from 720 to 930 cm (the deepest sample examined for *G. menardii*). Previous work has

a.

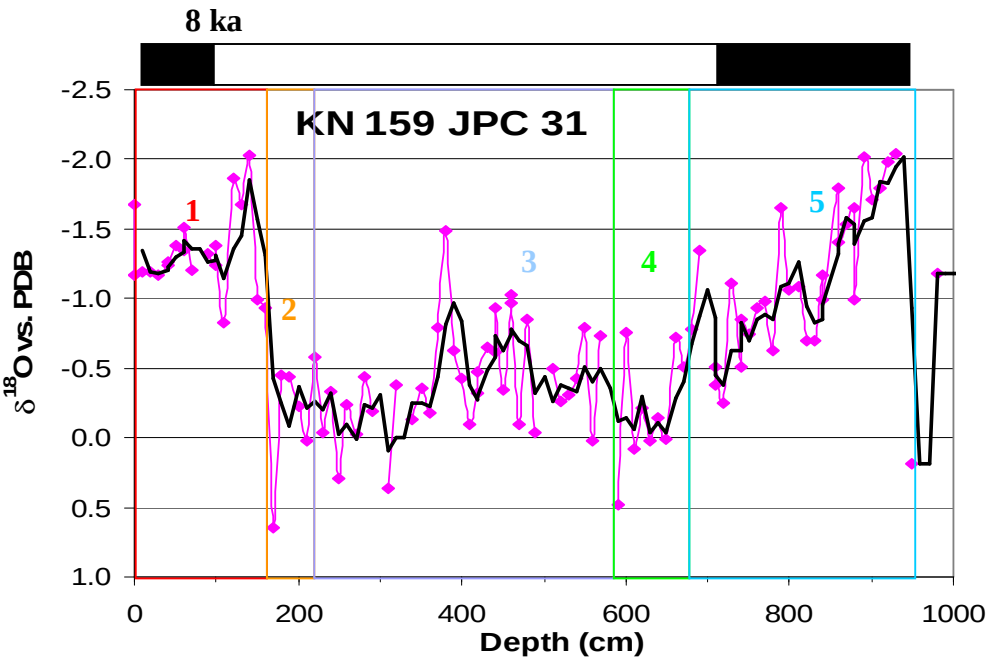

b.

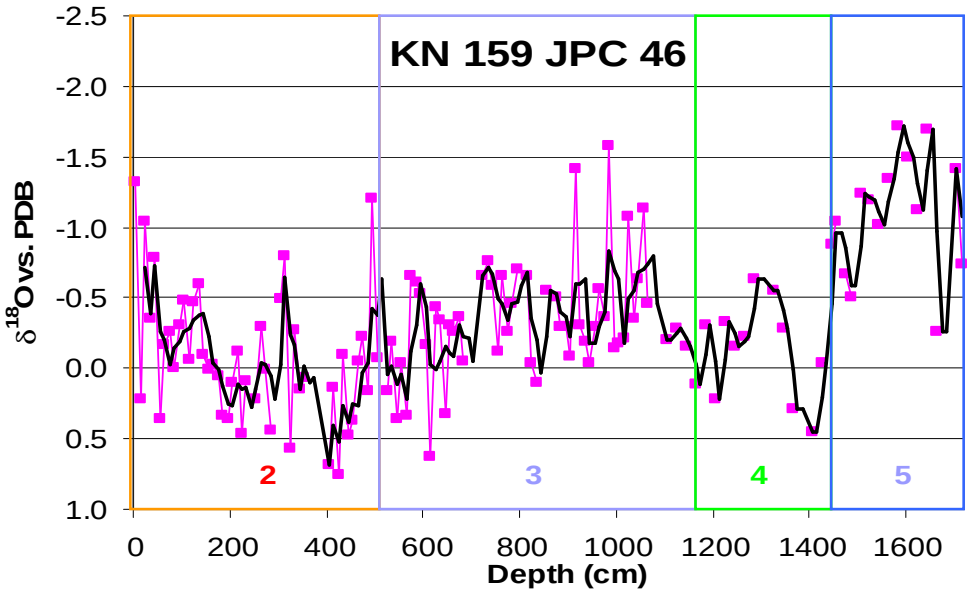

Figure 4: Results of $\delta^{18}O$ analysis of *G. ruber* from JPC 31 and 46. Numbers indicate marine isotope stage. Bar above graph represents presence (black) and absence (white) of *G. menardii* in JPC 31. Date of 8 ka obtained from G. A. Jones (1993, unpublished).

shown that in the Gulf of Mexico, *G. menardii* occur during the Holocene and last interglacial (MIS 5) but are absent during the last glaciation (MIS 2-4) (e.g., Ericson and Wollin, 1968; Emiliani, 1969). Thus, the positions of the MIS 1/2 and MIS 4/5 boundaries indicated by foraminiferal $\delta^{18}O$ are in accord with those indicated by *G. menardii*.

Ages obtained by radiocarbon dating of *G. ruber* and elemental analysis of volcanic ash deposits confirm the chronology for the upper 700 cm of JPC 31 (Figure 5, Table 1). The age of the sediments at 70-cm depth is 6,670 ± 60 yr BP, indicating that these sediments were indeed deposited during the early Holocene (MIS 1). The ages of sediments at 180 and 260 cm are 18,750 ± 290 yr BP and 21,750± 340 yr BP, respectively, confirming that these sediments were deposited during the last glacial maximum (MIS 2). Sediments at 680 cm are too old to yield an accurate radiocarbon date (>51,700 yr BP) as should be the case if they were deposited during the last interglacial (MIS 5).

The elemental composition of glass shards from the 2-cm thick ash layer at 700 cm depth in JPC 31 matches the composition of ash from the Los Chocoyos eruption from the Atitlan caldera in Guatemala (Table 2) (Hahn et al, 1979). The silica content of the shards is approximately 77%, indicating a rhyolitic to dacitic composition which averages ~65 to 78 % SiO_2 (Sarna-Wojcicki, 2000). Ash from the Los Chocoyos eruption is associated with ash layer Y8 in the northwestern Gulf of Mexico. According to Drexler (1980) this eruption took place at the isotopic stage 5a/b boundary and was given an age of 84,000 years. Figure 6 shows a picture of the glass shards analyzed.

The ages of the sediments in JPC 31 can be further constrained by *G. menardii* abundances and $\delta^{18}O$ profiles. Jones (1993) dated the most recent appearance of *G. menardii* into the Gulf of Mexico at 8 kyr; in JPC 31, the abundance of *G. menardii* increases abruptly between 90 and 100 cm (Figure 4), enabling us to assign an age of 8,000 yr BP to these sediments.

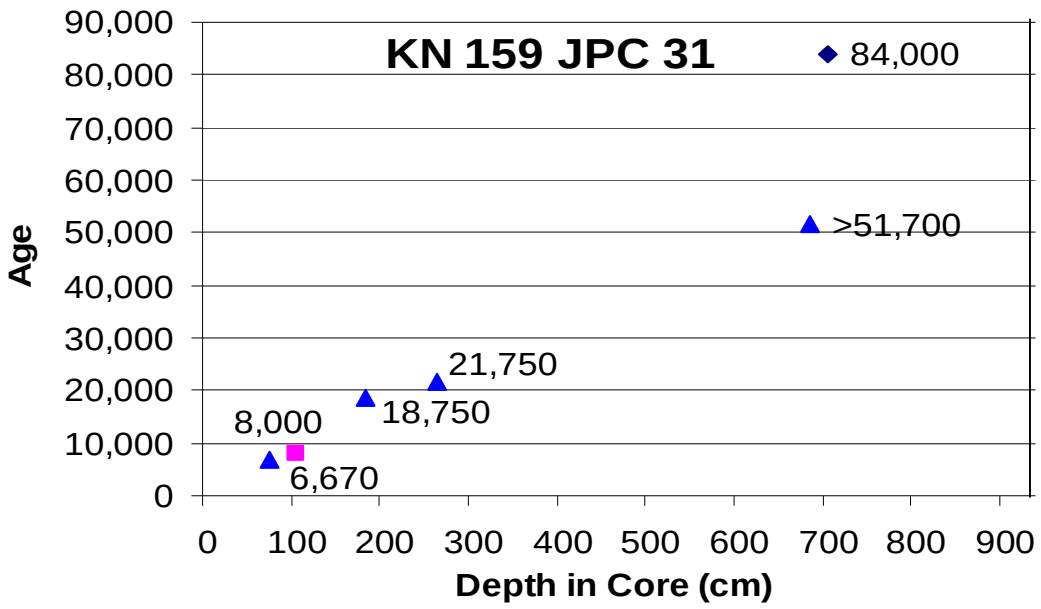

Figure 5: Summary of Three Dating Techniques. Age versus depth for JPC 31, based on *G. menardii* abundance (square), ^{14}C dating (triangles), and tephrochronology (diamond).

Table 1: Dates of Oxygen Isotopes and Radiocarbon Analysis. Ages are calendar years before present (1950) corrected for surface ocean reservoir effect (400 years).

Depth (cm)	Adjusted to Calendar Years
70	6,670
180	18,750
260	21,750
680	>51,700

Table 2: Results of Electron Microprobe Analysis. Chemical compositions of glass shards normalized for weight % oxide. Fe_2O_3 values were calculated from FeO and not directly measured. NA is "Not Analyzed".

Element	Avg. Composition for JPC 31 %	Normalized Avg. Composition for JPC 31 %	Avg. Composition for JPC 46 %	Normalized Avg. Composition for JPC 46 %	Normalized Composition for Y8 Los Chocoyos %
SiO_2	74.03	77.96	74.32	78.27	78.72
Na_2O	3.58	3.77	3.53	3.71	2.97
MgO	0.08	0.09	0.08	0.08	0.09
Al_2O_3	12.19	12.84	12.22	12.87	12.90
K_2O	3.74	3.94	3.93	4.14	3.98
CaO	0.61	0.64	0.59	0.62	0.63
TiO_2	0.09	0.10	0.09	0.09	0.08
Fe_2O_3	0.57	0.60	0.57	0.60	0.57
Cl	0.11	0.12	0.11	0.11	NA
Mn	NA	NA	NA	NA	0.07
Total	95.00	100.05	95.42	100.44	100.01

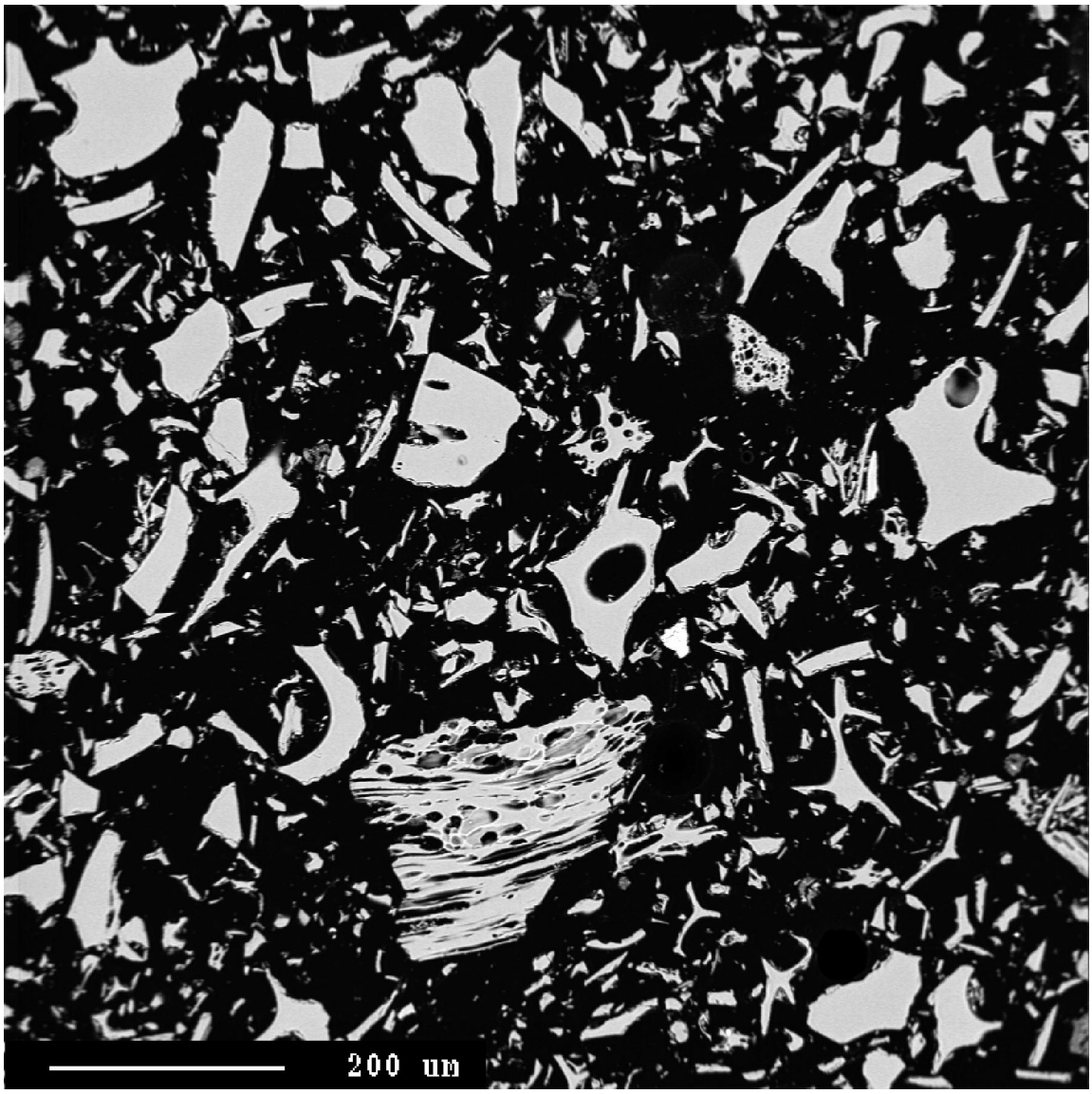

Figure 6: Photomicrograph of JPC 31 Glass Shards.

As discussed previously, the oxygen isotope values at the top of JPC 31 show Holocene values of approximately –1.3 ‰ (Figure 4). At approximately 110 cm, a single isotopic value approaches -0.5 ‰. This value hints at the presence of the pattern seen by Broecker et al. (1989) for the Younger Dryas Event. With a larger sampling resolution, the Younger Dryas Event may be seen. The Younger Dryas Event is generally accepted to have occurred between 11 and 10 kyr BP. At 140 cm the isotopic value is –2.03 ‰ and is the most negative isotopic value for the past 100,000 years, indicating a meltwater spike. As depth in the core increases, a steep increase in isotopic values is apparent. At 170 cm the oxygen isotope value is +0.64‰. This change in values is the most dramatic in JPC 31 and indicates the change from the Holocene to the Pleistocene epochs, as well as the change from oxygen isotope MIS 1 to MIS 2. Table 3 lists the depth of each stage in JPC 31 and JPC 46 and its age.

Sediment core JPC 31 shows isotopic patterns similar to those seen in other sediment cores for MIS 2, 3, and 4 from the Gulf of Mexico. As shown in several other analyses, the boundaries of MIS 2/3 and 3/4 are not as distinct due to the homogeneity of the isotopic values. Although these boundaries are not easily identified; nevertheless, we can recognize the pattern of isotopic value changes that typifies the last glaciation seen in other cores. Few specific conclusions can be made of the depths at which each of these stages occur; however, a general pattern of warmer and cooler temperatures can be interpreted. These three stages combined lasted approximately 60 ka. Because of the sharp isotopic change, the beginning of MIS 2 and the end of MIS 4 are easy to define. For the purpose of this paper, I have drawn approximate boundaries between these stages. MIS 2 begins at 150 cm and ends at 350 cm. MIS 3 begins at 350 cm and ends at 550 cm. MIS 4 begins at 550 cm and ends at 660 cm. The transition from MIS 4 to MIS 5 has been dated at 71 ka by SPECMAP (Imbrie et al, 1984).

MIS 5 is the last isotopic stage recorded in JPC 31. The pattern of oxygen isotopes in MIS 5 was so discernable that Emiliani divided this stage into five additional substages. These substages mimicked the glacial/ interglacial pattern observed in the large-scale patterns. Substages 5a and 5c, warmer periods, contained sediment thicknesses of approximately 70 cm. Substage 5a is given an age of 83.3 ± 0.3 ka (Gallup et al. 1994). Substage 5b and 5d were short and contained sediment thicknesses of 20-30 cm. The warmest Substage 5e, at 840-940 cm, is the thickest in MIS 5.

JPC 46

The downcore variations of $\delta^{18}O$ in JPC 46 are similar to those of JPC 31, though with a much higher resolution (Figure 4). Two relative maxima occur in JPC 46 at depths of 30-450 cm and 1140-1420 cm, and are MIS 2 and MIS 4, respectively. The top-most $\delta^{18}O$ in *G. ruber* are approximately –0.75 ‰ in JPC 46. This is in contrast to the Holocene values that averaged –1.3 ‰ in JPC 31. This suggests that JPC 46 does not contain the most recent Holocene sediments (likely not recovered by the piston core device). Table 4 shows the depth of each MIS boundary in JPC 46. The depositional period for the 9 m of sediments in JPC 31 is roughly equal to the 17 m of JPC 46 (MIS 1 to 5). The high resolution of this record allows the study of climate between glacial and interglacial periods.

The most recent oxygen isotope values for JPC 46 begin at approximately –0.75 ‰. These values are similar to the values of the transition from Holocene to Pleistocene in JPC 31, which is shown to be 12 ka (Shackleton, 2000). The transition from Pleistocene to Holocene is also the defined as the transition from MIS 2 to MIS 1.

Table 3: Depth of Isotopic Stages. ND is "Not Determined". Sources: SPECMAP (Imbrie et al, 1984); Martinson et al. (1987); and Gallup et al. (1994).

MIS Stage	Boundary Depth in JPC 31 (cm)	Boundary Depth in JPC 46 (cm)	U/Th Dating of Coral, Speleotherms, and Sediments (ka)	SPECMAP (ka)
1/2	150	30	11.5	11
2/3	250	450	ND	ND
3/4	550	1140	ND	ND
4/5	660	1420	79.7	71
5a/5b	710	1460	83.3	100
5b/5c	730	1490	ND	ND
5c/5d	810	1610	ND	ND
5d/5e	840	1630	117	115
5e/6	930	1650	>130	128

The oxygen isotope values continue to increase as the glacial period of the Pleistocene continues. A gradual decrease in approximately the first 30 cm of JPC 46 are MIS 1.

Again, the boundaries of MIS 3 are not easily defined. MIS 2 starts at 30 cm and MIS 4 ends at 1420 cm. The MIS1/2 boundary is generally accepted to have an age of 12 kyr. The MIS 4/5 boundary has been shown to have an age of 72 kyr (Imbrie et al, 1984; Winograd et al., 1992, Slowey et al., 1996). Therefore 1390 cm of sediments in JCP 46 comprise this time span of 60 kyr. In order to better create a chronostratigraphic framework, the boundaries of MIS 3 were estimated. The definition of each isotopic stage and its values can be seen in Figure 4b. MIS 5 is the earliest isotopic stage recorded in JPC 46. Substage 5a is given an age of 83.3 ± 0.3 ka (Gallup et al., 1994). Substage 5e, dated approximately 123 kyr by Slowey et al., (1996) Imbrie et al. (1984), and Gallup et al., (1994), begins at 1640 cm.

Late Quaternary Sedimentation Rates

The chronologies of JPC 31 and JPC 46 provide a framework with which to consider sedimentation rates along the slope of the northwest Gulf of Mexico during the late Quaternary. Cores collected during the Knorr 159 cruise display similar density profiles as discussed previously and as seen in Figure 8. Downcore variations in density may have several causes, including grain size and carbonate/clay ratio. However, regardless of the cause of the change, it is most important that correlation is possible. This figure shows the correlation of the chronologies developed for cores 31 and 46 and comparison with the other cores. By directly correlating oxygen isotope stages with density, a density signature may be established for some events. The MIS 1/2 and 4/5 boundaries, as well as the Y8 ash layer, are visible on the density profiles. Based on their density profiles (not shown for all cores), from northwest to southeast (Fig. 2), the following cores were used to examine sedimentation rates to the northwestern slope of the Gulf of Mexico: JPC 19, JPC 20, JPC 18, JPC 46, JPC 22, JPC 28, JPC 23, JPC 16, JPC 31, JPC 24, JPC 26, and JPC 34. These cores were divided by depositional environment: Upper Slope (JPC 19, JPC 20, JPC 18,

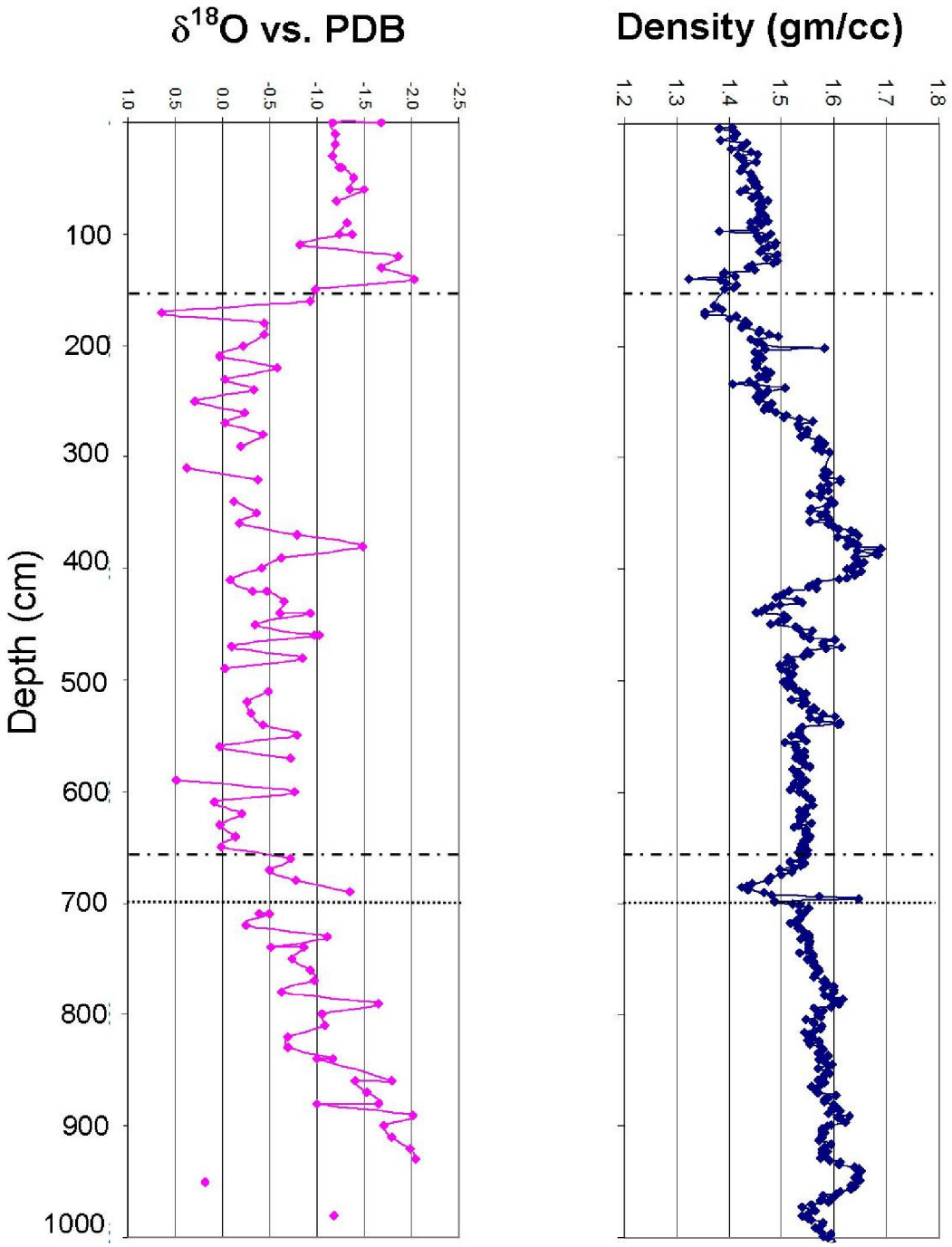

Figure 7: Density and $\delta^{18}O$ Correlation of JPC 31.

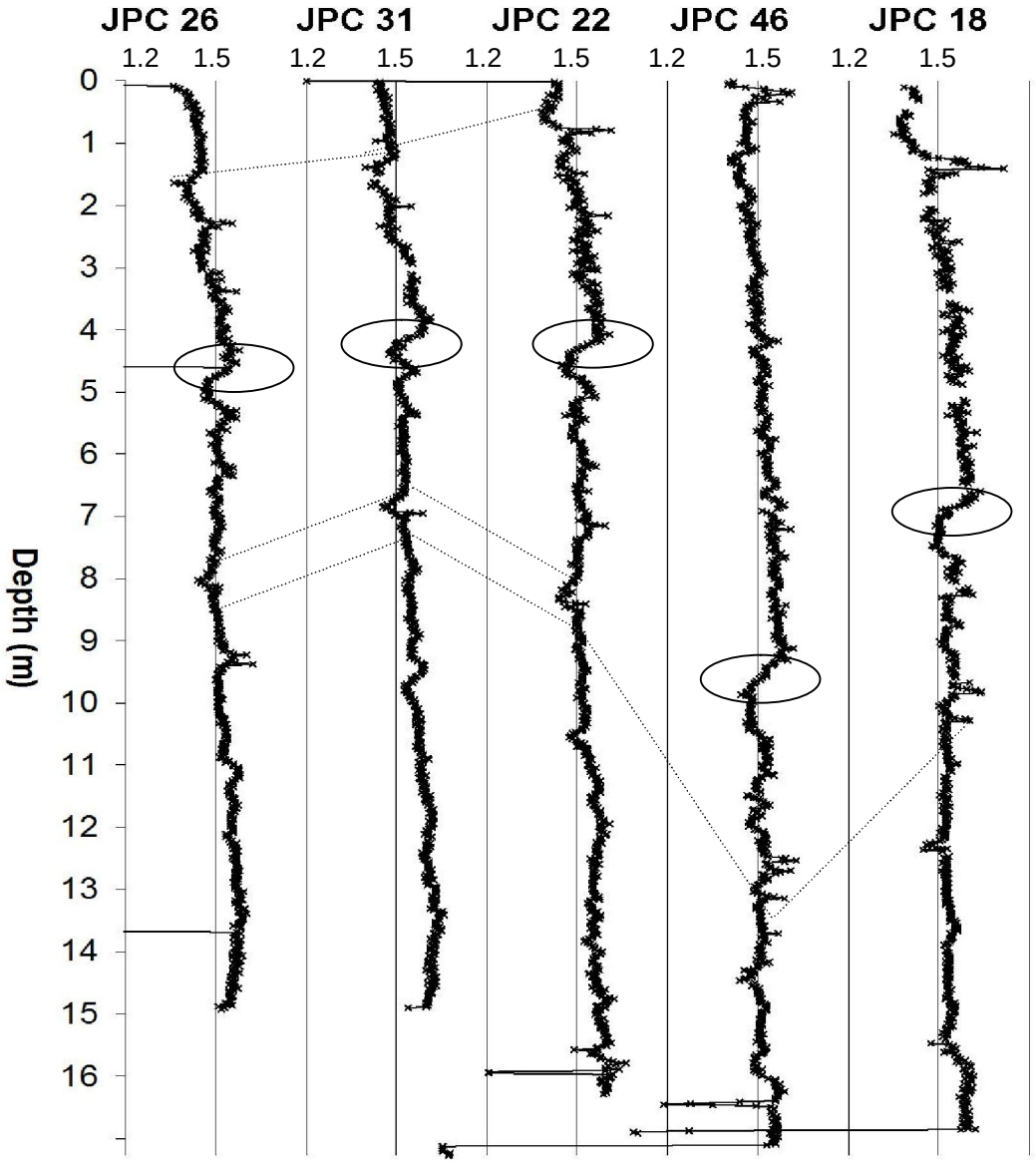

Figure 8: Density Profiles and Correlation of Select Cores. Correlations drawn to demonstrate density signatures across cores. The circle represents a decrease in density used to correlate.

and JPC 46), Mid-Slope (JPC 22, JPC 28, JPC 23, and JPC 16), and Lower Slope (JPC 31, JPC 24, JPC 26 and JPC 34). Table 4 and Figure 8 show the locations and calculated sedimentation rates for each of these cores. Table 5 gives sedimentation rates for each of the above cores for each MIS identified in the density profile.

During the Holocene, sedimentation rates based on density profiles on the Upper Slope were approximately 7 cm/1000 yr. The sedimentation rates for the Holocene on the Mid Slope were approximately 9 cm/ 1000 yr, and Lower Slope rates were approximately 12 cm/ 1000 yr. Normal sedimentation rates for the slope of the Gulf of Mexico during the Holocene are between 5 cm/1000 yr and 10 cm/1000 yr. Sedimentation rates are usually expected to decrease from the Upper to Lower Slope due to a decrease in sediments carried by rivers; however this "inverted" pattern of sedimentation rates is likely due to high speed bottom currents that occurred during the high sea level stand (Hamilton and Lugo-Fernandez, 2001). The sedimentation rates for the slope are average for an interglacial period with hemi-pelagic sediments.

The Stage 2/3 boundary, as well as the Stage 3/4 boundary, lack density signatures, and are therefore difficult to identify from core to core in the northwestern slope. A decrease in density was noted in each density profile and ranged in depth from 260 cm to 1230 cm among the cores analyzed (shown in Figure 9). The age for this feature was calculated using the age boundaries of MIS 3, which were 60 to 24 kyr. The age of this feature is 42 kyr. This feature divides Stage 3 into two substages: MIS 3a and MIS 3b. In MIS 3a, the sedimentation rates are much higher and more variable. The reason for this drastic change in density and sedimentation in the middle of a steady climate is unknown. This could be due to a high sand content distributed to the slope through high river discharges during variable climates. Another possibility is the washing out of sediments deposited in MIS 3 during the low sea level stand of MIS 2. The Upper Slope has an approximate sedimentation rate of 26 cm/1000 yr.

Table 4: Location of Cores and Sedimentation Rates.

Area	**Core**	**Latitude (Degrees)**	**Longitude (Degrees)**	**Sedimentation Rate (cm/kyr)**
Upper Slope	JPC 19	27.54	-92.48	28
	JPC 20	27.54	-92.48	21
	JPC 18	27.14	-92.38	15
	JPC 46	27.06	-92.34	17
Mid Slope	JPC 22	26.90	-92.40	11
	JPC 28	26.86	-92.26	14
	JPC 23	26.76	-92.34	7
	JPC 16	26.77	-92.23	11
Lower Slope	JPC 31	26.42	-92.20	8
	JPC 24	26.38	-92.19	7
	JPC 26	26.38	-92.04	10
	JPC 34	26.11	-91.95	14

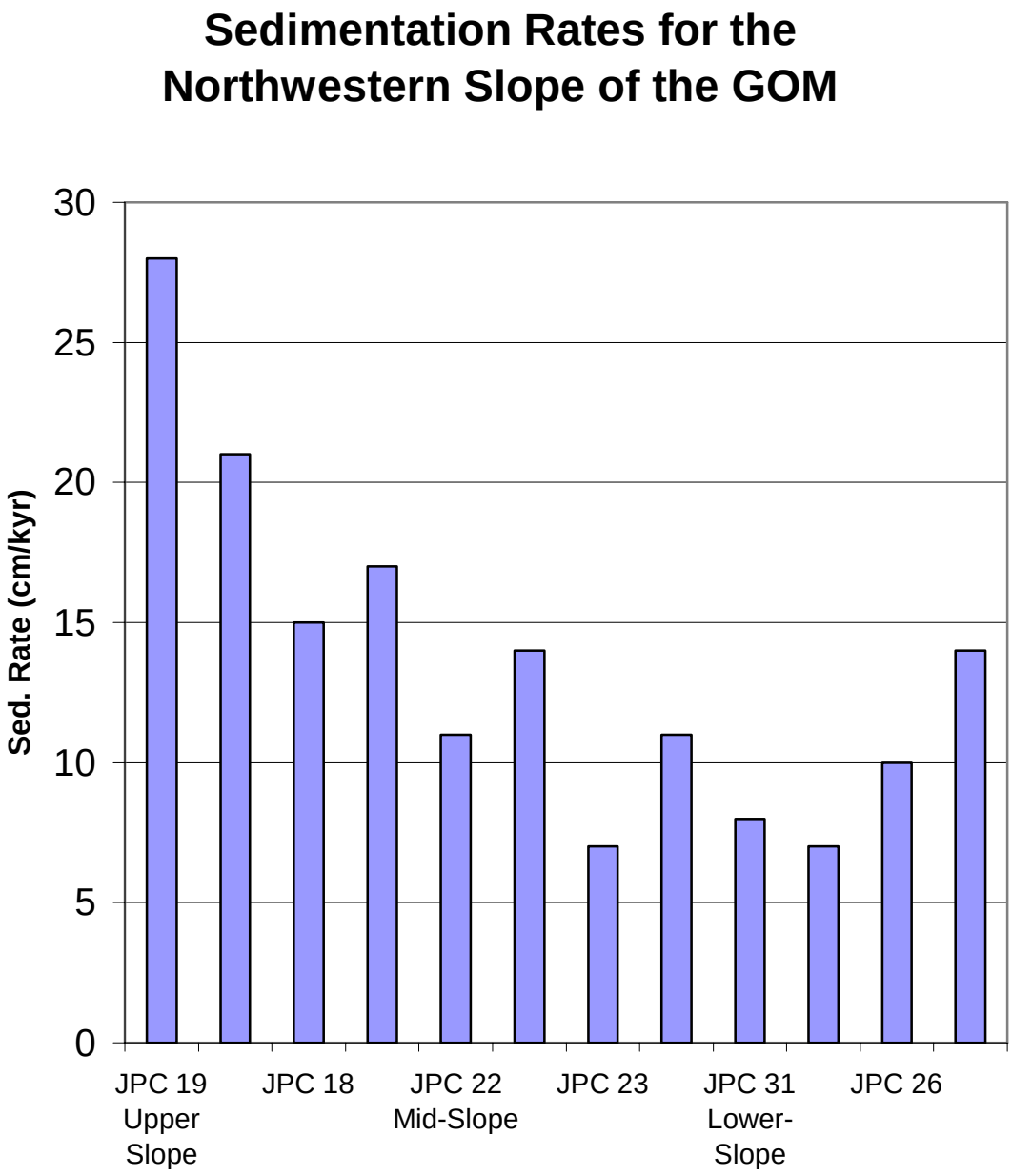

Figure 9: A Bar Diagram of Sedimentation Rates of Select Cores. Rates are calculated for the last 120,000 years.

Table 5: Sedimentation Rates of Each Core. Bold denotes cores correlated with oxygen isotope data.

Core	**Stage 1 Sed. Rate (0-10.5 cm/kyr)**	**Stage 2/3/4 Sed. Rate (10.5-72 cm/kyr)**	**Stage 5a Sed. Rate (72-84 cm/kyr)**
JPC 19	NA	NA	NA
JPC 20	NA	NA	4.2
JPC 18	6.7	18.9	5.0
JPC 46	**2.9**	**22.0**	**5.0**
JPC 22	NA	NA	3.3
JPC 28	8.6	16.4	3.3
JPC 23	7.6	7.2	2.5
JPC 16	NA	NA	3.3
JPC 31	**15.2**	**8.0**	**4.2**
JPC 24	6.7	7.8	2.5
JPC 26	16.2	9.8	2.5
JPC 34	NA	NA	NA

The Mid and Lower Slopes have similar sedimentation rates of 13 and 11 cm/kyr, respectively. This is the expected pattern of decreasing sedimentation rates towards the Lower Slope, which is a function of distance from fluvial sources. The increasing sedimentation rates toward the bottom of the lower slope likely reflect deposition by turbidity currents.

The MIS 4/5 boundary, which marks the transition from interglacial to glacial climate, was difficult to define in the cores; however, this boundary was marked by a slight increase in density, as shown in the oxygen isotope and density correlation of JPC 31 (Figure 7). The age of this boundary is 72 ka according to Gallup et al (1994) or 71 ka according to Imbrie et al. (SPECMAP, 1984). Sedimentation rates for MIS 5 ranged from 15 cm/kyr at the Upper Slope to 9 cm/kyr at the Lower Slope. This is the expected pattern of decreasing sedimentation rates towards the Lower Slope, which is a function of river introduced sediments and turbidity currents. These sedimentation rates are slightly lower than those noted during the density drop; however, this is due to the low sea level stand during MIS 2, which carried an extraordinary amount of sediments out to the Gulf of Mexico.

The final density signature noted in all of the density profiles examined is the small increase in density due to the presence of an ash layer. This ash layer, Y8, dated at 84,000 years, is present during MIS 5a. Sedimentation rates were relatively uniform across the slope, and only varied from 4 to 6 cm/kyr. These sedimentation rates are typical for hemi-pelagic sediments in an interglacial period.

CHAPTER IV
CONCLUSION

The objective of this study was to develop an age model to correlate stratigraphy across the northwestern slope of the Gulf of Mexico. This chronostratigraphy was then used to study sediment deposition rates along the slope as a function of climate change. We used oxygen isotope stratigraphy to determine general climate patterns and correlate ages with other studies. With tephrochronology, we identified one ash layer in both cores and analyzed the chemical composition for specific elements to obtain an absolute date of 84,000 years. We used radiocarbon dating at four depths in JPC 31 to obtain absolute dates for correlation. Foraminiferal abundances of *G. menardii* provided another absolute date of 8,000 years. We identified five marine isotope stages that date back to 120 kyr BP. In JPC 31, all five marine isotope stages were present within the first 9 m of the core. In JPC 46, the first stage (MIS 1) was not present; however, the remaining four marine isotope stages were observed in the 17 m core. By applying ages to the physical properties of the sediments, both climatic and geologic events can be identified and more easily understood.

Sedimentation rates on the northwestern slope of the Gulf of Mexico ranged from 7 cm/kyr to 28 cm/kyr for the most recent 120,000 years. Holocene sedimentation rates were lower than the above and ranged from 3 cm/kyr to 16 cm/ kyr. The sedimentation rate for the last glaciation (MIS 2, 3, and 4) had the highest sedimentation rates for the time analyzed. The lowered sea level during the glacial advance brings sediments farther out onto the slope; therefore, a higher sedimentation rate is expected during this time. These rates varied from 22 cm/kyr near the coast to 7 cm/kyr toward the abyssal plains. Sedimentation rates for MIS 5a (72 – 84 kyr) ranged from 5 cm/kyr to 25 cm/kyr. After comparing sedimentation rates for each of the 12 cores analyzed along the slope, JPC 23 and JPC 24 had the lowest rates in most comparisons. This is likely due to high density bottom currents and turbidity currents which carry sediments farther out the slope.

REFERENCES

Amery, G., 1969. Structure of the Sigsbee Scarp, Gulf of Mexico. American Association of Petroleum Geologists Bulletin, 53, 2480-2482.

Arnold, J. R., Anderson, E. C., 1957. The distribution of carbon-14 in nature. Tellus, 9, 28-32.

Bard, E., 1988. Correction of accerlerator mass spectrometry 14C ages measured in planktonic foraminifera: Paleoceanographic implications. Paleoceanography, 3 (6), 635-645.

Bouma, A.H. and Bryant, W. R., 1994. Physiographic features on the northern Gulf of Mexico continental slope. Geo-Marine Letters. 14, 252-263.

Broecker, W.S., Kennet, J.P, Flower, B.P., Teller, J.T., Trumbore, S., Bonani, G., Wolfli, W., 1989. Routing of meltwater from the Laurentide Ice Sheet during the Younger Dryas cold episode. Nature, 341, 318-321.

Bryant, W.R., Liu, J. Y., and Ponthier, J., 1995. The engineering and geological constraints of intraslope basins and submarine canyons of the northwestern Gulf of Mexico. Gulf Coast Association of Geological Societies Transactions, 45, 95-101.

Bryant, W., Liu, J.Y., 2000. Deep water program, Gulf of Mexico deep water information resources data search and literature synthesis, OCS Study, MMS-00-19, Narative Report: Geology, pp. 3-1 to 3-34.

Craig, H., 1957. Isotopic standards for carbon and oxygen and correction factors for mass spectrometric analysis of CO2. Geochim. Cosmochim. Acta., 12, 133-149.

Crowley, T., North, G.R. Paleoclimatology. New York, Oxford University Press, New York, 339 pp, 1991.

Curry, W. B., Matthews, R. K., 1980. Equilibrium 18O fractionation in small size fraction plaktonic foraminifera: Evidence from recent Indian Ocean sediments. Marine Micropaleontology, 6, 327-337.

Emiliani, C. 1955. Pleistocene temperatures. Journal of Geology, 63, 538 – 578.

Emiliani, C. 1969. A new paleontology. Micropaleontology, 15, 265-300.

Emiliani, C. 1975. Paleoclimatological analysis of late quaternary cores for the northeastern Gulf of Mexico. Science, 26, 1083-1088.

Ericson, D.B., Wollin, G., 1968. Pleistocene climates and chronology in deep-sea sediments. Science. 162 (3859), 1227-1234.

Fairbanks, R.G., 1989. A 17,000-year glacio-eustatic sea level record: Influence of glacial melting rates on the Younger Dryas event and deep-ocean circulation. Nature, 342, 637-642.

Flower, B.P., Kennett, J. P., 1990. The Younger Dryas cool episode in the Gulf of Mexico. Paleoceanography. 5 (6), 949-961.

Gallup, C.D., Edwards, R.L., Johnson, R.G., 1994. The timing of high sea levels over the past 200,000 years. Science, 263, 796-800.

Gealy, B. 1955. Topography of the continental slope in the northwest slope of the Gulf of Mexico. Bulletin of the Geological Society of America, 66, 203-228.

Hahn, G.A., Rose, W. I, Meyers, T., 1979. Geochemical correlation of genetically related rhyolitic ash-flow and airfall ashes, central and western Guatemala and the Equatorial Pacific. G.S.A. Spec. Paper 180, Ash Flow Tuffs, ed. by W. Elston and C. Chapin, 100-114.

Hamilton, P., Lugo-Fernandez, A. 2001. Observations of high speed deep currents in the northern Gulf of Mexico. Geophysical Research Letters, 28, 2867 – 2870.

Imbrie, J., Hays, J.D., Martinson, D.G., McIntyre, A., Mix, A.C., Morley, J.J., Pisias, N.G., Prell, W.L., Shackleton, N.J., 1984. The orbital theory of Pleistocene climate: Support from a revised chronology of the marine $\delta^{18}O$ record. In: Berger, A., Imbrie, J., Hays, J., Kukla, G., Saltzman, B. (Eds.), Milankovitch and Climate Part I, NATO ASI Series C, Mathematical and Physical Sciences. D. Reidel Publishing Co, Dordrecht, Netherlands, pp. 269-305.

Jones, G.A., 1993. Timing of the Holocene repopulation of the Atlantic Ocean by *G. menardii* and *G. tumida* and implications for surface watermass paleoceanography. Accepted by Deep-Sea Research. Unpublished.

Martin, R. E., Johnson, G. W., Neff, E. D., Krantz, D. W., 1990. Quaternary planktonic foraminiferal assemblage zones of the northeast Gulf of Mexico, Colombia Basin (Caribbean Sea), and tropical Atlantic Ocean: Graphic correlation of microfossil and oxygen isotope datums. Paleoceanography, 5, 531-555.

Martinson, D. G., Pisias, N. G., Hays, J. D., Imbrie, J., Moore, T. C., Jr., Shackleton, N. J., 1987. Dating and the orbital theory of the ice ages: Development of a high-resolution 0 to 300,000-year chronostratigraphy. Quaternary Research, 27, 1-29.

Rabek, K., Ledbetter, M.T., Williams, D.F., 1985. Tephrochronology of the western Gulf of Mexico for the last 185,000 years. Quaternary Research, 23, 403- 416.

Ruddiman, W. F., Raymo, M., McIntyre, A., 1986. Matuyama 41,000-year cycles: North Atlantic Ocean and northern hemisphere ice sheets. Earth and Planetary Science Letters, 80, 117-129.

Sarna-Wojcicki, A., 2000. Tephrochronology, In: Noler, J. S., Sowers, J. J., Lettis, W. R. eds., Quaternary Geochronology: Methods and Applications: American Geophysical Union, Washington DC, pp. 357–377.

Shackleton, N.J., Opdyke, N.D., 1973. Oxygen isotope and paleomagnetic stratigraphy of equatorial Pacific core V28-238: Oxygen isotope temperatures and ice volumes 10^5 year and 10^6 year scale. Quaternary Research, 3, 39-55.

Shackleton, N.J., 2000. The 100,000-year ice-age cycle identified and found to lag tempearture, carbon dioxide, and orbital eccentricity. Science, 289, 1897-1902.

Slowey, N.C., Henderson, G.M., Curry, W.B., 1996. Direct U-Th dating of marine sediments from the two most recent interglacial periods. Nature, 383, 242-244.

Stuiver, M., Polach, H. A., 1977. Discussion: Reporting of 14C data. Radiocarbon, 19 (3), 355-363.

Suess, H. E. and Revelle, R. R., 1957. Carbon dioxide exchange between atmosphere and ocean and the question of an increase of atmospheric CO_2 during the past decades. Tellus, 9, 18-27.

Winograd, I.J., Coplen T.B., Landwehr, J.M., Riggs, A.C., Ludwig,K.R., Szabo, B.J., Kolesar, P.T., Revesz, K.M., 1992, Continuous 500,000-year climate record from vein calcite in Devils Hole, Nevada. Science, 258, 255-260.

VITA

Kristen Eileen Elston

Mailing Address:	1802 Heather Cove Ct, Houston, Texas 77062.
Telephone:	(281) 330-0189 (cell).
Education:	B.S., Texas A&M University, (Geography) 1998. M.S., Texas A&M University (Oceanography), expected 2005.
Experience:	01/1999 to 12/2000 – Teaching Assistant, Department of Oceanography, Texas A&M University, College Station, Texas. 05/1997 to 01/1999 – Research Assistant, Department of Oceanography, Texas A&M University, College Station, Texas.